NASA Project Mercury Working Paper No. 231

DESIGN STUDY OF A METEOROID EXPERIMENT

USING AN UNMANNED MERCURY SPACECRAFT

NATIONAL AERONAUTICS AND SPACE ADMINISTRATION

MANNED SPACECRAFT CENTER

Houston, Texas

December 27, 1962

DESIGN STUDY OF A METEOROID EXPERIMENT

USING AN UNMANNED MERCURY SPACECRAFT

NATIONAL AERONAUTICS AND SPACE ADMINISTRATION

MANNED SPACECRAFT CENTER

Houston, Texas

December 27, 1962

DESIGN STUDY OF A METEOROID EXPERIMENT

USING AN UNMANNED MERCURY SPACECRAFT

Prepared by: _____
Leslie G. St.Leger
Head, Structural Analysis Section

Authorized for Distribution:

_____
Maxime A. Faget
Assistant Director, Engineering and Development

NATIONAL AERONAUTICS AND SPACE ADMINISTRATION

MANNED SPACECRAFT CENTER

Houston, Texas

December 27, 1962

TABLE OF CONTENTS

LIST OF FIGURES

LIST OF TABLES

INTRODUCTION

A need exists for meteoroid data which is directly applicable to the design of vehicles for long-duration space flight. Experiments to obtain this data must be of relatively long duration, must be unmanned, must involve relatively large exposed areas, and must have the capability of being recovered for examination.

The Mercury spacecraft and its concept of reentry and recovery have been proven in numerous orbital flights. This spacecraft has the capability of operating unmanned and has the largest weight-carrying ability of any such space vehicle available to date.

The purpose of this paper is to present the results of a preliminary study of a meteoroid experiment and carrier vehicle based upon the Mercury spacecraft. The study has been carried out in sufficient detail only to highlight the principal problems involved, and to present a discussion of these problems upon which a decision as to the feasibility and desirability of such a vehicle might be based.

Included in this paper is a brief historical account of the currently available meteoroid information, and some of the controversial aspects associated with it.

EXISTING METEOROID ENVIRONMENT DATA

The hazard imposed by extra-terrestial debris on space vehicles necessitates the definition of the distribution, size, and velocity of meteoroids in space. Although the observation of meteors entering the earth's atmosphere dates back to the nineteenth century, the science of meteor astronomy really began with Whipple's use of twin cameras instituted in the Harvard Meteor Program in 1936. This, together with the techniques of radio astronomy introduced in 1946, and some very limited satellite data, form the basis of all existing knowledge relating to meteoroid activity in the near-earth vicinity. At greater distances from the earth, little or nothing is known about meteoroid activity.

Astronomical Data

Astronomers are in general agreement that all observed meteors emanate from within the solar system, and that no less than 90 percent of the total number are of cometary origin. The remaining 10 percent

are classified as being of asteroidal origin, the asteroids being a belt of planetary debris which orbit the sun between the planets Mars and Jupiter.

Meteors are further classified as "sporadics" or "showers". Showers occur regularly during the course of the year and are characterized by a sharp increase in meteor activity. This variation in meteor activity throughout the year is illustrated in figure 1 which is reproduced from reference 1. Because of the short duration of each major shower, their contribution to the total annual flux is considerably less than that due to sporadic activity. The distribution of meteoroid orbits are concentrated at or near the earth-sun ecliptic plane. This distribution which has been confirmed in recent years by radio-echo techniques is illustrated in figure 2. Approximately 80 percent of the total flux is confined to within ±25° of the ecliptic plane.

The total number of meteoroids entering the earth's atmosphere is usually plotted as a function of "visual magnitude"; which is a logarithmic scale used by astronomers based on light intensity step ratios of $(100)^{1/5}$ or 2.512. The reference point of the visual magnitude scale is taken as 1.0 and represents the average light intensity as observed by the naked eye, of the twenty brightest stars. The visual magnitude scale is inverted in that an increase in visual magnitude number represents a decrease in brightness. Although the naked eye cannot perceive a light intensity less than +5.0 on the visual magnitude scale, the term is retained as a matter of convenience. The daily mean number of meteoroids of a given visual magnitude and greater, entering the earth's atmosphere per day, is shown plotted in figure 3.

Meteoroid Mass

All astronomical observations result in data relating to meteor velocity, luminosity, and orbital characteristics. The concept of meteoroid mass and density which are also required for an analysis of the meteoroid hazard to space vehicles must be obtained by mathematical deduction or satellite experiments. Two fundamental relationships may be used to obtain the meteoroid mass and density. One expression is that which relates the conversion of kinetic energy into light and is written:

$$I = \frac{\beta}{2} \frac{dm}{dt} V^2$$

where

I = light intensity, ergs per second

V = meteor velocity (1)

$$\beta = \text{luminous efficiency,} \quad \frac{\text{ergs. sec.}^2}{\text{gm.cm.}}$$

$$\frac{dm}{dt} = \text{rate of mass loss}$$

Assuming the total mass of the meteoroid to be consumed during atmospheric entry, and assuming the velocity to be sensibly constant, the above equation can be integrated to give the meteoroid mass:

$$m = \frac{2}{V^2 \beta} \int_c^t I \, dt \qquad (2)$$

In the above expression, V and I are measurable quantities, but the factor for the luminous efficiency is not easy to evaluate, and estimates given in reference 8 vary by two orders of magnitude from .0002 to .02.

The second relationship that may be used to estimate the meteoroid mass is the aerodynamic drag expression:

$$D = \frac{1}{2} C_D \cdot S \cdot V^2 = m\frac{dv}{dt} \qquad (3)$$

and, by substitution, assuming a spherical particle this equation reduces to:

$$m^{1/3} \cdot \rho_m^{2/3} = \frac{1.21 C_D \cdot \rho \cdot V^2}{(dv/dt)} \qquad (4)$$

where   m = meteoroid mass

C_D = hypersonic drag coefficient

ρ = atmospheric density

ρ_m = density of meteoroid particle

S = cross-sectional area

$\frac{dv}{dt}$ = deceleration.

The deceleration and meteoroid velocity are obtained from observation, and the atmospheric density and drag coefficient assuming a

spherical shape are known sufficiently well. However, in order to
solve equation (4) for the meteoroid mass, an impossible assumption as
to the meteoroid density must be made.

Various investigators have derived estimates of meteoroid mass-
number relationship using the luminous intensity expression given in
equation (2). The results of two of these investigators, Whipple and
Watson, are shown in figure 4, and the spread in results is essentially
due to different values assumed for the luminosity coefficient. Also
shown in this figure are some experimental results obtained from earth-
orbiting satellites, using acoustic impact detectors. The conversion
of these microphone measurements of meteoroid impacts to individual
particle mass introduces the uncertainty of whether the pulse voltage
obtained by impact is proportional to momentum, or energy, and also
requires an assumption regarding the impact velocity.

Meteoroid Velocity Relationship

Since the advent of photographic techniques, it has been possible
to measure meteor velocities by placing two cameras a relatively large
distance apart. However, the sensitivity of the film has restricted
the data to a relatively large size range between visual magnitudes
0 to +5. The average of these observed velocities is 28 km/sec. Whipple,
in reference 4, deduces that the very small particles of visual magni-
tude 20 and greater have much lower velocities of the order of 15 km/sec,
and assumes a linear variation of velocity between the two, as shown in
table 1.

Meteoroid Densities

Estimates of meteoroid density range from a very low value of
.05 gm/cc based on the assumption that meteoroids of cometary origin
are composed of a loose aggregate of particles with a very low overall
density; to a high value of 7.8 gm/cc for meteoroids of asteroidal
origin. Fred Jonah in reference 5 has made an attempt to correlate
meteoroid densities with atmospheric density, using the drag equation,
and the correlation based on the model atmosphere of reference 6 is
shown in figure 5. The results indicate that a density of .3 gm/cc
can be assigned to the larger fast-moving meteoroids, while a density
of 4.0 gm/cc gives good correlation for the smaller particles which
burn up at lower altitudes. He therefore suggests that up to visual
magnitude 15, a meteoroid density of .3gm/cc be used, and a density of
4.0 gm/cc be used for visual magnitude greater than 20. An alternate
proposal by Whipple in reference 7 is that the following expression be
used to obtain meteoroid density:

$$\log \rho_m = -1.03 - .214 \log m$$

where

$$\rho_m = \text{meteoroid density, -gm/cc} \qquad (5)$$

and m = meteoroid mass, grams

This relationship gives a high value of 8.0 gm/cc for the very small particles which are a few microns in diameter, and a density of .05 g/cc for the large particles of visual magnitude zero. A comparison of these estimated densities is shown in figure 6.

METEOROID EXPERIMENT

Required Experimental Data

The purpose of any meteoroid experiment should be to obtain a better definition of the meteoroid flux, and a better assessment of the damage to be expected on typical spacecraft structures. Available data, obtained from ground observations are limited to the flux covering a mass range of 10^{-3} to 10^{-1} grams, while the experimental data obtained from earth-orbiting satellites has been confined in an extremely low mass range of 10^{-10} to 10^{-7} grams. Unfortunately, this data is at the two extreme ends of the mass scale, and does not cover the mass range of interest for the penetration of typical spacecraft structures. This area of interest is shown in figure 4 and interpolation of the flux data into this area of interest has led to a great deal of controversy. Since the weight of spacecraft structures is greatly dependent on the meteoroid environment assumed, it is essential that an attempt be made to obtain an accurate estimate to the flux and mass distribution.

This dependence of structural weight with various assumed meteoroid environments is illustrated in figure 7 for a typical spacecraft structure, such as the shell of the Apollo Service Module. If a severe meteoroid environment is assumed, with a meteoroid density of 3.5 g/cc, then in order to attain a reliability of the order of .99 which is required for manned missions, a structural weight penalty of 400 pounds above the required for strength provisions is imposed. This mushrooms into a total payload penalty of approximately 1000 pounds for the Apollo L.O.R. mission assuming a specific impulse of 315 seconds for the hypergolic propellant in the service module. If the meteoroid environment does turn out to be of this severe a nature, then it should be known very accurately, since any errors in the data would lead to either a further increase in shielding weight, or a loss of reliability. If, on the other hand, the meteoroid environment agrees more with Watson's suggestions and the meteoroid density is as low as .3 gm/cc, then any inaccuracies in

the data would not be too significant since the weight of the structure is then dictated by strength requirements.

A meteoroid experiment, to be of practical use to the spacecraft designer, should, ideally, produce the following data:

a. The flux versus mass of the meteoroid population for meteoroids in the mass range 10^{-7} to 10^{-2} grams. This is the mass range that would penetrate typical spacecraft structures as shown in figure 4.

b. The velocity variation with meteoroid mass.

c. Meteoroid density.

d. The penetration resistance of typical structures.

All four of the above objectives can only be met by an extensive and sophisticated family of experiments. However, the first objective and some insight into the other phases of the problems can be accomplished by the use of a single mission using an unmanned Mercury spacecraft. This experiment would be designed to yield:

a. The total number of impacts on an exposed sheet during a specified orbit lifetime. This data would be used to confirm the meteoroid flux in the extremely small mass range as presently obtained from other satellites. Telemetered instrumentation would be required to obtain this information.

b. The total number of penetrations experienced by an exposed sheet during a given time. The sheet thickness chosen would be designed for penetrations by meteoroids having a mass greater than 10^{-7} grams. This information would be obtained by both telemetry and/or post-recovery inspection.

Statistical Problem

In order that a single experiment be made to produce useful results, it is essential that a significant number of data points be obtained from the one experiment. The ultimate objective of a Mercury meteoroid experiment is to obtain penetration information that can be incorporated into the design of manned spacecraft, and the ideal way to do this would be to utilize a typical Apollo-type structure for the experiment. However, since these structures are designed with a high reliability of the order of .99, the area-time product required for penetration data would be prohibitively large.

Most Probable Number of Penetrations

By the selection of a suitable material thickness, the experiment
may be designed to yield a large number, such as one hundred probable
penetrations, or a relatively small number such as ten. If a large
number is selected, the probability of obtaining within 5 percent of
the most probable number of one hundred penetrations is relatively high,
of the order of 40 percent, and the chance of getting a significantly
different number from one hundred is relatively small. If, on the other
hand, the experiment is designed to yield a small number of penetrations
of the order of ten, then the probability of obtaining within 5 percent
of that number is only about 12 percent and the probability curve is
quite flat so that the probability of getting numbers widely different
to 10 remains close to 12 percent. These thoughts are illustrated in
figure 8, which shows the histograms for most probable numbers of one
hundred, and ten, respectively.

Due to large variance of opinion regarding the meteoroid flux and
density, the experiment should be designed to yield around one hundred
as the most probable number of penetrations when based on the mose severe
environment assumptions. Hence, if a large number is in fact recorded,
the information could be regarded as accurate, and if a low number is
recorded, it can be attributed to a less severe environment than that
assumed, and not to statistical variations.

Thickness and Exposure Time Required

An ideal experiment would consist of exposing a typical spacecraft
structure to the environment. A typical effective single sheet thickness
of Apollo Service Module is 0.17 inches. Using this thickness of alu-
minimum for a meteoroid experiment that would produce one hundred pene-
trations based on a severe environment assumption would require an area-
time product of 10^7 ft^2 days, as illustrated in figure 9. This product
is four orders of magnitude greater than the area-time product of a
single Apollo mission, and is impossible to achieve.

The area-time product that appears more feasible for a Mercury
meteoroid experiment is about 30,000 ft^2 days. In order to maintain
an expected number of penetrations of one hundred, when based on the
Whipple Flux, and a meteoroid density of 3.5/cc, the thickness of the
aluminum sheet used in the experiment must be no greater than .016 inches.

Relationship Between Material Thickness and Meteoroid Mass

The mass of a meteoroid that will penetrate a sheet is a function
of the sheet thickness and the material properties. A reduction in the

sheet thickness to be used for the experiment by one order of magnitude from 0.17 inches which is typical of manned spacecraft structures, to 0.016 inches means a reduction of three orders of magnitude in the mass of the penetrating type meteoroid from 10^{-4} grams to 10^{-7} grams, as shown in table II. This mass is just about at the upper limit of that being recorded by satellite and rocket probes.

Hence the constraints of area-time product, the weight and volume limitations of the Mercury-Atlas vehicle, and practical engineering considerations make possible the attainment of meteoroid data only at the lower limit of the mass range of interest for practical structures. (Fig. 4)

EXPERIMENTAL VEHICLE

General Description and Concept

The experimental payload would consist basically of a single aluminum sheet, .016 inches thick which would be preformed and heat-treated to a tubular shape, and deployed aft during orbit through the cylindrical section of the Mercury capsule. An artist's concept of the sheet in the extended position is shown in figure 10. In the stored position within the spacecraft, the sheet would be wound on a drum as a flat coiled ribbon. This concept has been successfully demonstrated with small diameter tubes used as deployable antennas on the Canadian "Top Side Sounder" that was recently launched in a polar orbit. It appears analytically feasible to use the same principle for larger diameters, but no doubt some development time would be required.

Details of Experimental Payload

Storage of coiled sheet within the spacecraft.- In order to effect a satisfactory C. G. location for floatation stability, it is necessary to remove the couch-support beams so that the coiled sheet can be installed as low down as possible within the spacecraft as shown in figure 11.

The maximum length of sheet that can be coiled on a spool using a 6 inch diameter mandrel is approximately 1800 feet. The maximum width of sheet that can be deployed through the recovery compartment is 26 inches, which results in a tubular diameter of 8.0 inches when deployed, and gives an exposed surface area of 3500 ft^2. The size of the spool with the coiled sheet is approximately 30 inches wide, with an outside diameter of 38 inches. It is not possible to install a package of this size through either of the escape hatches; therefore

the large pressure bulkhead must be detached for installation and postflight removal.

Deployment and Retraction

Deployment and retraction of the aluminum sheet during orbit is effected by two electric motors. One motor located near the junction of the cylindrical and conical sections of the spacecraft is used to drive a pair of rollers which deploys the sheet, and the other is used to drive the drum during retraction. This arrangement results in the flat length of sheet between the rollers and the drum always being kept in tension.

Spacecraft Modifications

In order to keep the spacecraft weight to a minimum, and to deploy the sheet through the recovery compartment, the spacecraft will be stripped of all unnecessary equipment, and certain major modifications which are summarized below will be necessary.

a. Remove antenna canister.

b. Relocate drogue parachute and mortar within recovery compartment.

c. Retain only one main parachute.

d. Redesign reaction-control system.

e. Relocate pitch and yaw scanners in conical section.

f. Remove small pressure bulkhead.

g. Remove seat-support beams.

Instrumentation

Since the spacecraft will be recovered after the experiment, the number and location of meteoroid penetrations of the sheet may be determined by a detailed postflight inspection. However, in order to assess the meteoroid environment, the total number of meteoroid impacts must also be known. This can only be done with instrumentation which either telemeters the information back to earth by ground command, or stores the information on magnetic tape on board the spacecraft.

The most suitable type of instrumentation consists of mylar foil with a very thin film of aluminum deposited on one surface. This foil,

which has a total thickness of the order of .0003 inches, is cemented
to both sides of the deployed sheet, and acts as a recuperable capitance
gauge when connected to the terminals of the onboard batteries. Although
this type of instrumentation has not yet been used for any flight experi-
ments, it has been extensively laboratory tested, and has the virtue of
being able to record the total number of meteoroid impacts, as well as
the total number of sheet penetrations.

Weight and Center of Gravity

Figure 12 shows a weight breakdown for the configuration proposed
for the experiment. The maximum height of the C. G. required for water
stability is 120 inches and this has been attained by installing the
coiled sheet as low down as possible within the spacecraft. The total
launch weight of the spacecraft is approximately 3000 pounds and the
landing weight 2400 pounds. The landing bag has been included in the
weight summary since it is desirable to maintain relatively low
water-impact decelerations on the concentrated mass of spool and coiled
sheet within the spacecraft.

The weight indicated for the attitude-control system is based on
a hypergolic system, since this system must be redesigned to control
angular rates which are much higher than currently exist.

Strength and Stiffness Requirements

Because of the variation in angular velocities during extension
and retraction, associated Coriolis accelerations are imposed on the
sheet which are a function of the deployment and retraction rates, with
the retraction condition being by far the most critical. Because of
the relatively thin gauge of sheet being used, the bending stresses in-
duced by these accelerations must be kept quite small in order to pre-
vent buckling of the sheet. Figure 16 shows that in order to prevent
buckling, the retraction rates for a sheet that is 1800 feet long must
be less than one inch per second at the start of retraction and may be
increased because of the relief afforded by the centrifugal force as
the sheet gets shorter to a maximum of 3.5 in/sec. Using this variable
rate of retraction, the total time required for retraction is 335 minutes
which is equivalent to $3\frac{1}{2}$ orbits.

Deflected Shape of Sheet

The bending moment induced in the sheet during retraction will
cause the sheet to assume a deflected shape as shown in figure 17.
However, because the stresses in the sheet must necessarily be kept
very low to prevent buckling, the maximum deflection at the tip is

not unduly large.   For a sheet length of 1800 feet the maximum tip deflection with respect to the C. G. is approximately 4.0 feet.

OPERATIONAL CONSIDERATIONS

Orbital Lifetime

The preceding calculations on impacts and penetrations are based on the premise that an orbital lifetime of at least fourteen days can be achieved for the experiment when the length of exposed sheet is 1800 feet.   This would give an area-time product of approximately 30,000 ft^2 days when an earth shielding factor of 0.5 is included. Figure 13 indicates the predicted lifetime for circular orbits that can be achieved with the present Atlas launch vehicle.   With an exposed sheet length of 1800 feet, the predicted altitude for circular orbit is 123 nautical miles and the orbital lifetime is three days. Reducing the length of sheet to 700 feet has the effect of increasing the lifetime to nine days which is still less than the minimum desired.

In order, therefore, to achieve a satisfactory lifetime, an elliptical orbit with a perigee insertion altitude of 87 nautical miles is recommended.   The expected orbital lifetime for this condition is shown in figure 14, from which it may be seen that even allowing for large errors in the computations, a lifetime of fourteen days can be achieved with a sheet length of 1800 feet.   An insertion altitude of 87 nautical miles has been chosen in order to comply with the Atlas guidance system presently being used for the manned Mercury missions. The expected apogee for this condition is 400 nautical miles.

Tumbling Phenomena

During the major portion of the time in orbit, the attitude control system will be switched off and the spacecraft allowed to drift.   When the aluminum sheet is extended after insertion into orbit, the moment of inertia increases, and according to conservation of momentum principles, angular velocities will decrease.   During re-traction of the sheet, the reverse is true, and the angular velocity will increase.   Assuming an initial angular velocity of 4 degrees per minute at the start of retraction, figure 15 shows the increase in angular velocity as the sheet retracts, neglecting the effects of any gravitational gradient.   With the proposed 1800 feet long sheet, the terminal angular velocity reaches a value of 50 radians per second which must be damped out prior to reentry.

Attitude Control

The sequence of operation for the attitude control system will be as follows:

a. Immediately after orbital insertion the rate-damp mode will be employed to reduce the rates about all three axes to ±0.5 degrees per second.

b. The system will then be shut off and the spacecraft allowed to drift for fourteen days with the sheet deployed.

c. After retraction of the sheet, the rate-damp mode will again be employed to reduce angular rates to ±0.5 degrees per second about all three axes.

d. Prior to retro-fire a vertical attitude will be acquired, with no attitude control about the roll axis.

e. During reentry a programed roll rate of 10 degrees per second will be used to reduce dispersion of the landing area. The present Mercury reaction-control system will not be used for this experiment because of the storage problems associated with H_2O_2 for a fourteen day mission. A completely redesigned system employing either compressed nitrogen gas, or hypergolic propellants is suggested instead.

Retro-fire Attitude

A unique feature of the reaction control system is the vertical retro-fire attitude shown in figure 18, with the retro-rockets being fired in salvo to achieve reentry. The advantage of this procedure is that attitude control is required about two axes only, with no attitude control requirements about the roll axis.

CONCLUDING REMARKS

A meteoroid experiment using an unmanned Mercury spacecraft has been investigated and appears to be feasible. However, because of the constraints of the area-time product, and material thickness, the penetration data will be confined to the masses of the order of 10^{-7} grams, whereas information regarding meteoroids in the mass range 10^{-4} to 10^{-6} grams would be more applicable to typical spacecraft structures.

The main problems associated with the design of the experiment are the development time that will be required to prove the feasibility of using a preformed tubular cross-section that can be coiled flat on a drum, and the redesign required for the reaction-control system to cope with the high angular rates anticipated. Installation and removal of the drum will require the removal of the large pressure bulkhead, but no other major difficulties are foreseen.

REFERENCES

1. A. C. B. Lovell. Meteor Astronomy. Oxford Clarendon Press, 1954.

2. F. G. Watson. Between the Planets. The Blakiston Co., Philadelphia, 1941.

3. G. S. Hawkins and E. K. L. Upton. The Influx Rates of Meteors in the Earth's Atmosphere. Astrophysical Journal No. 128, 1958.

4. F. L. Whipple, Vistas in Astronautics. Pergamon Press, 1958.

5. F. C. Jonah. Critical Analysis of Solid Debris in Space. 1.Ae.S. Paper No. 60-73, 1960.

6. J. B. Hartung and W. C. Wetmore. A Composite Model Atmosphere for use in Project Mercury. N.A.S.A. working paper No. 205, 1960.

7. F. L. Whipple. The Medical and Biological Aspects of the Energies in Space. Columbia University Press, 1961.

8. F. L. Whipple. Physics and Medicine of the Upper Atmosphere. University of New Mexico Press, 1952.
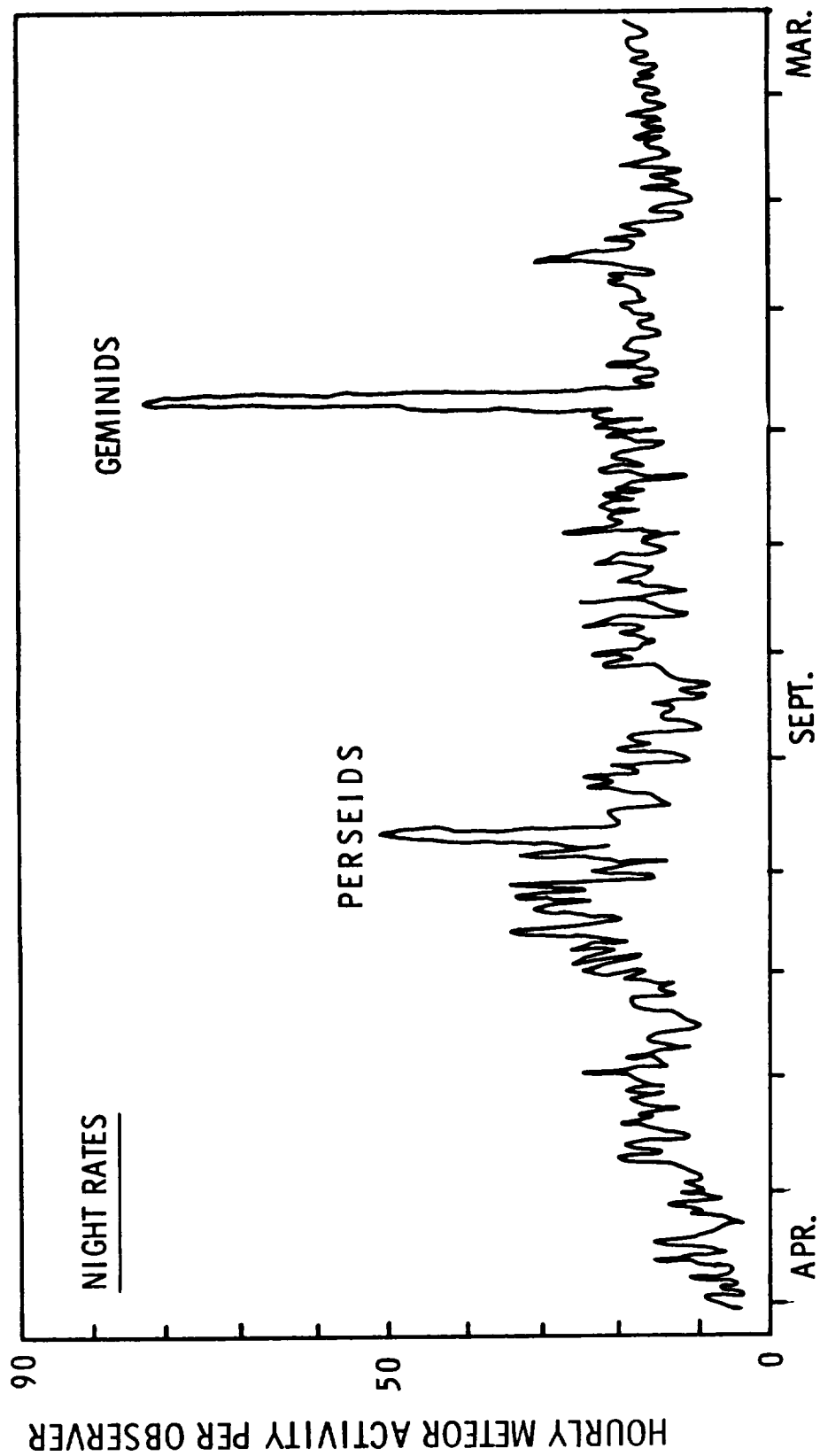
Figure 1.   Variation of meteor activity during the year

Figure 1. Concluded – Variation of meteor activity during the year

16
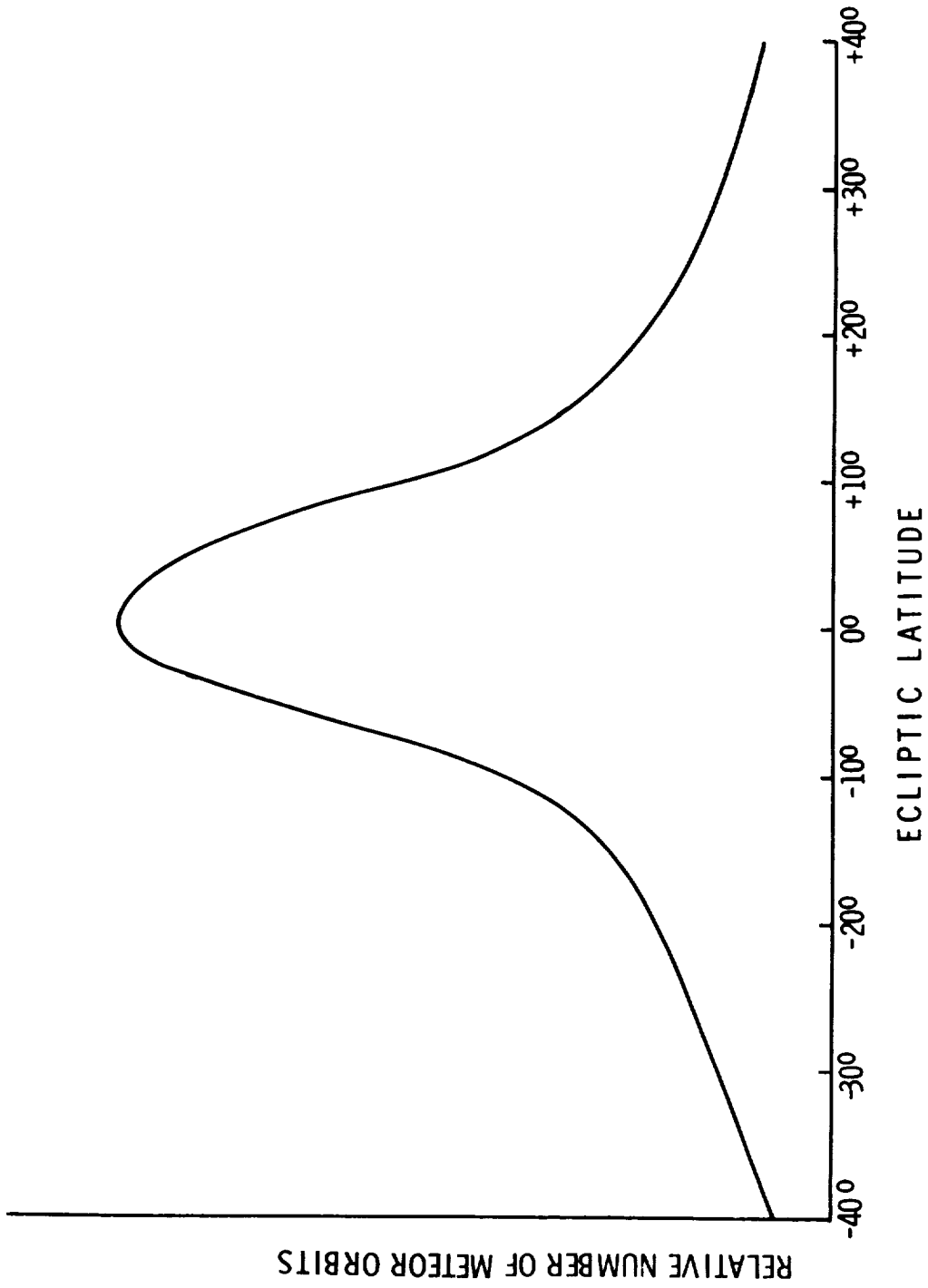

RELATIVE NUMBER OF METEOR ORBITS

ECLIPTIC LATITUDE

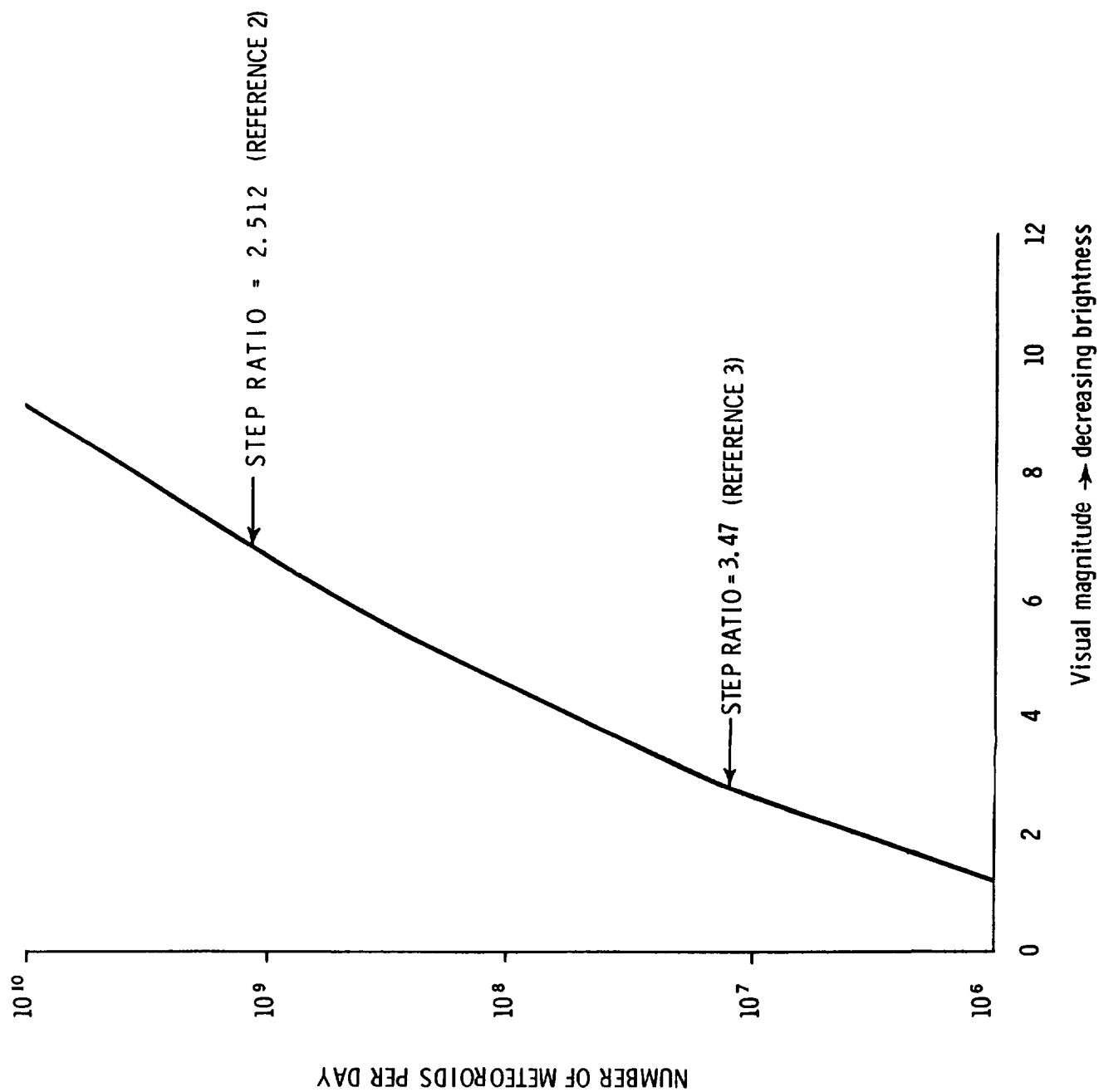Figure 2.   Inclination of meteor orbits relative to the earth's ecliptic plane

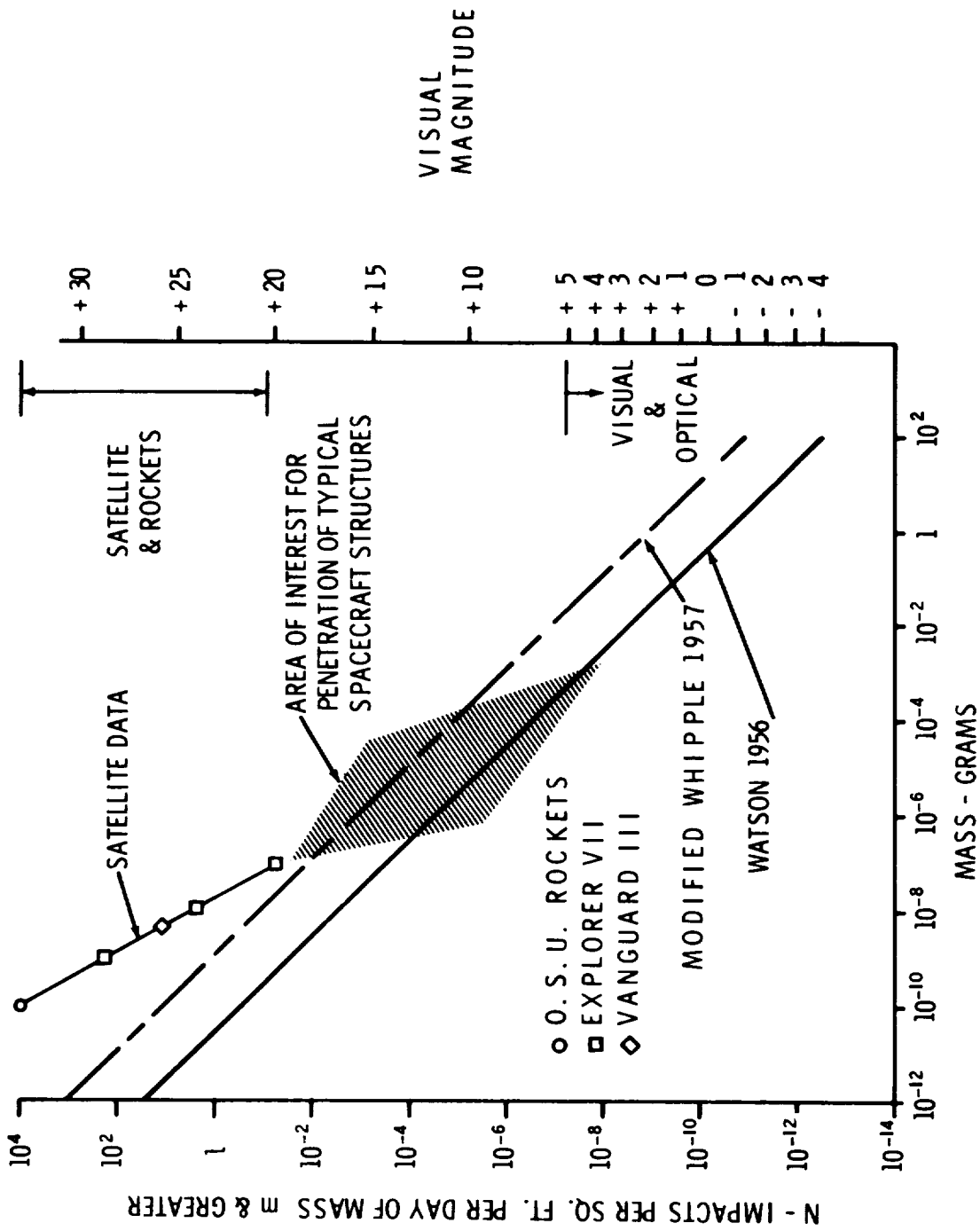Figure 3. Daily average of meteors entering earth's atmosphere.

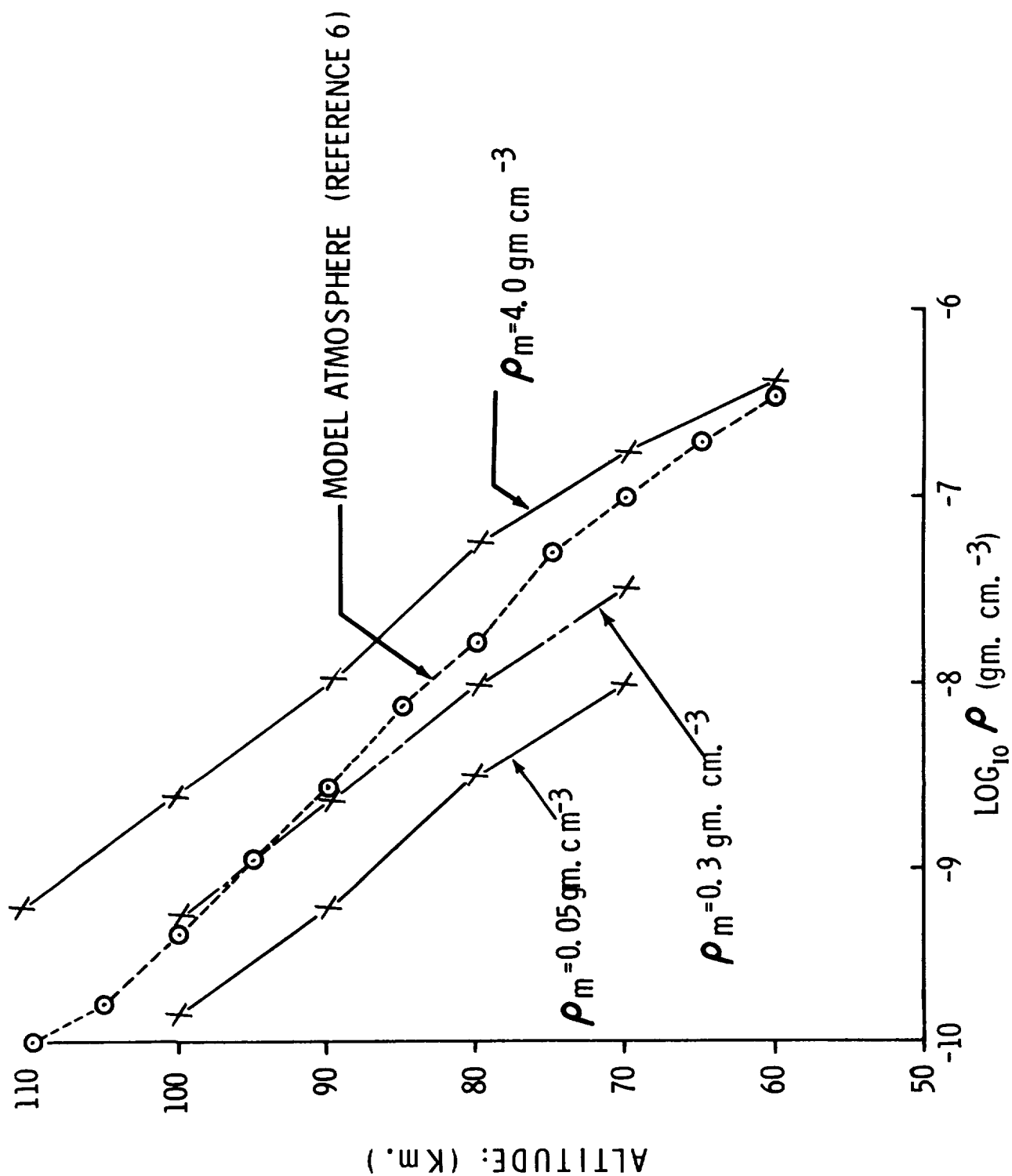Figure 4.   Flux-mass relationship of meteors entering the earth's atmosphere

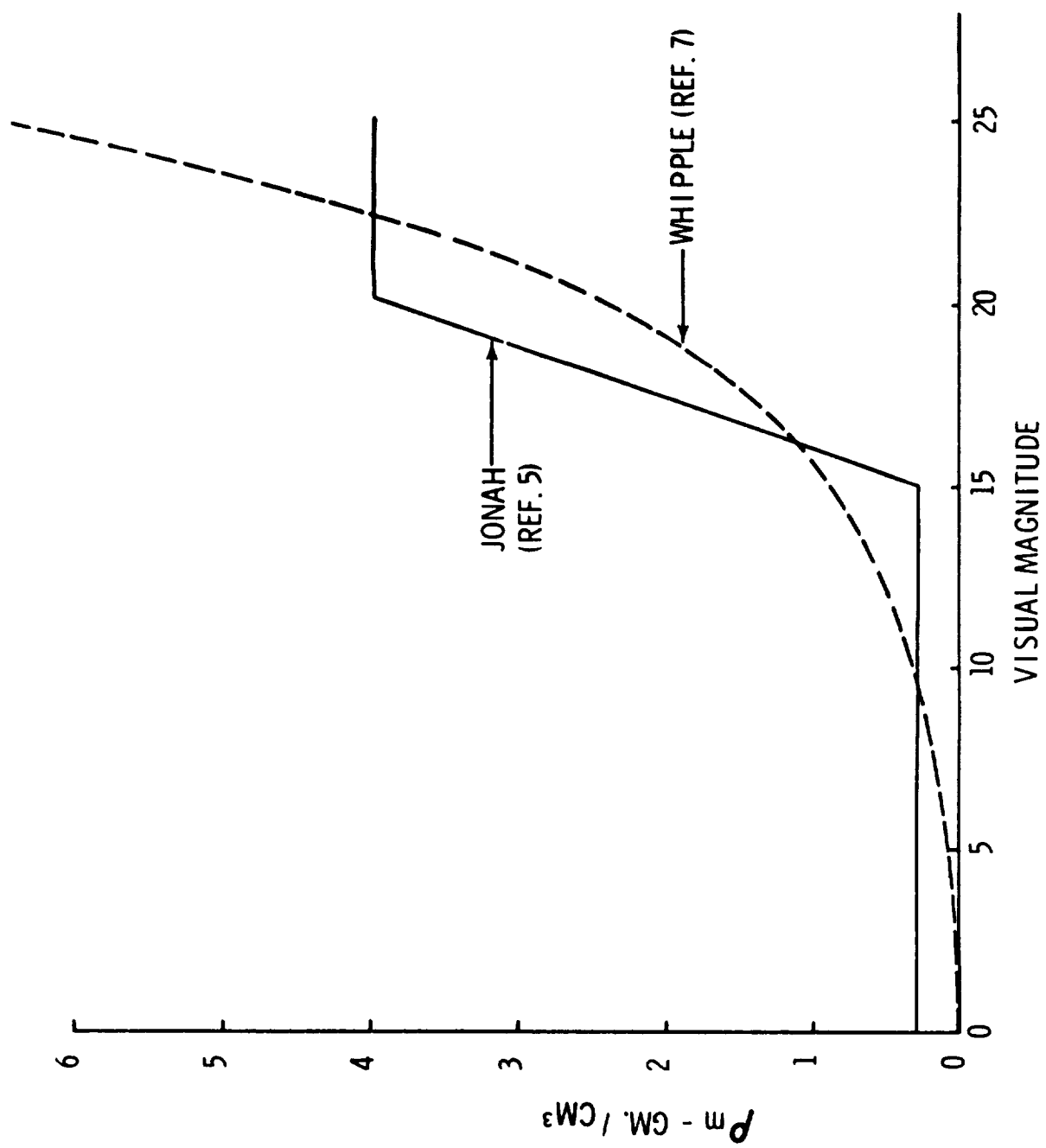Figure 5.   Correlation of atmospheric density derived from assumed meteoroid density

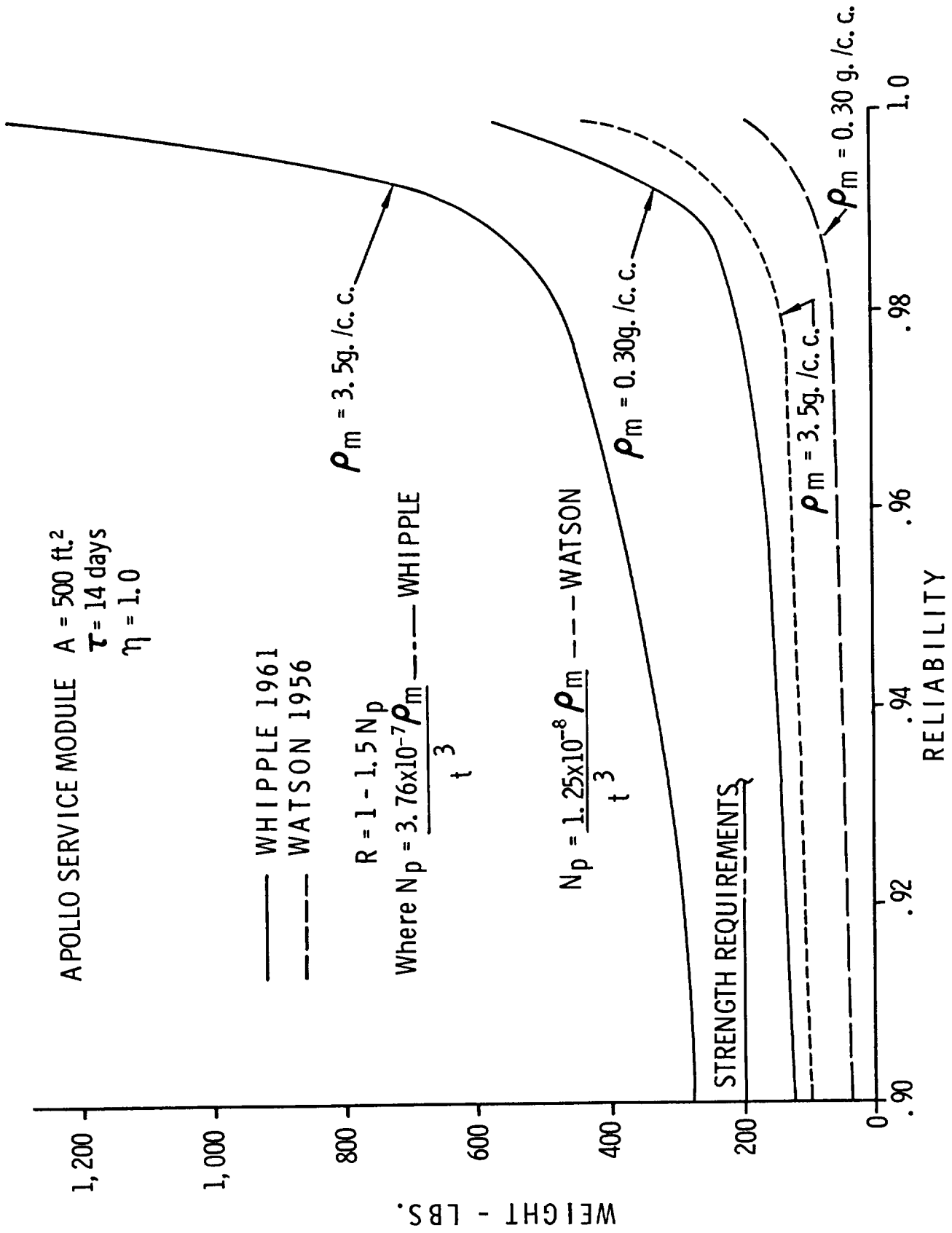Figure 6.   Meteoroid densities as proposed in referneces 5 & 7

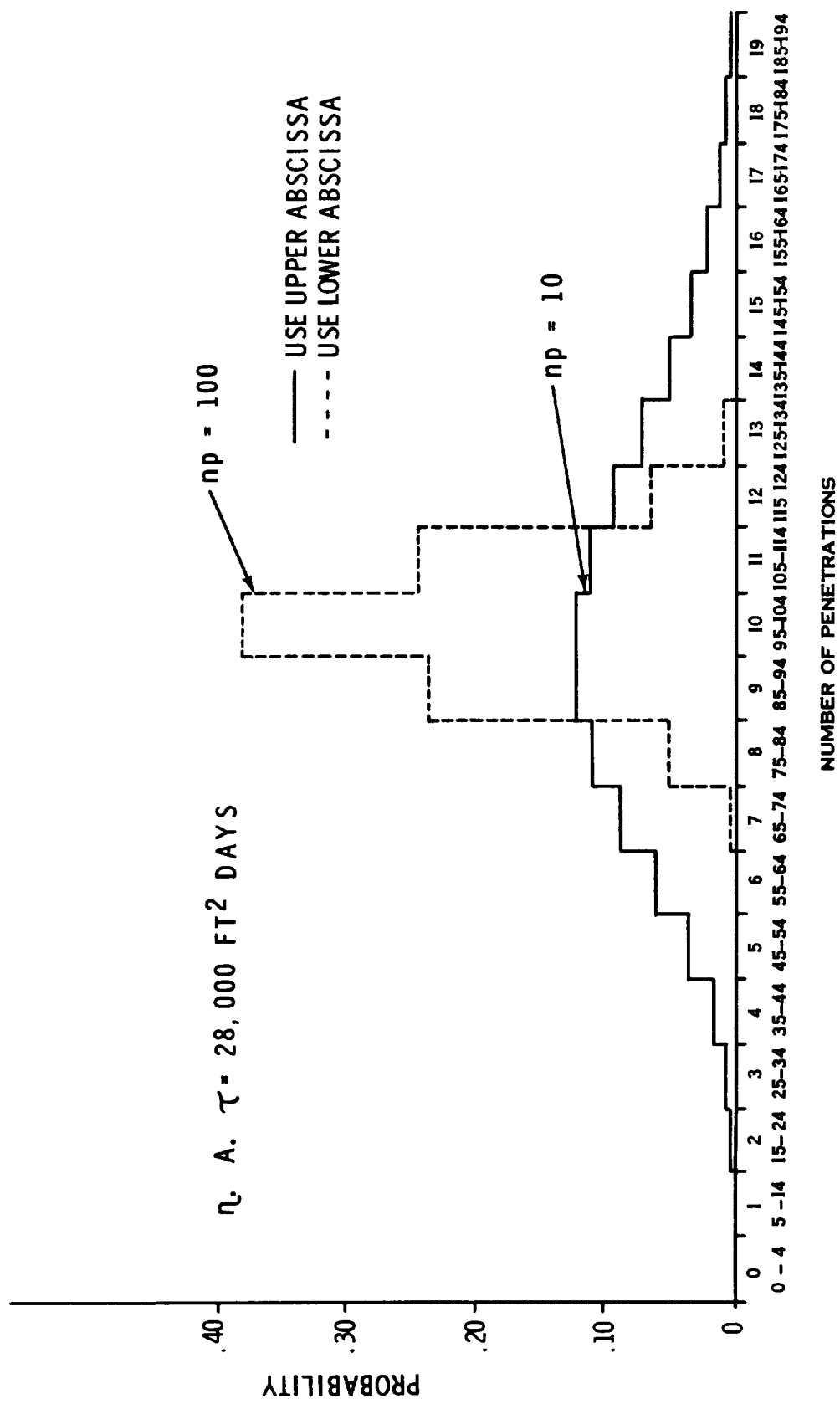Figure 7. Effect of meteoroid environment assumptions on shielding weight.

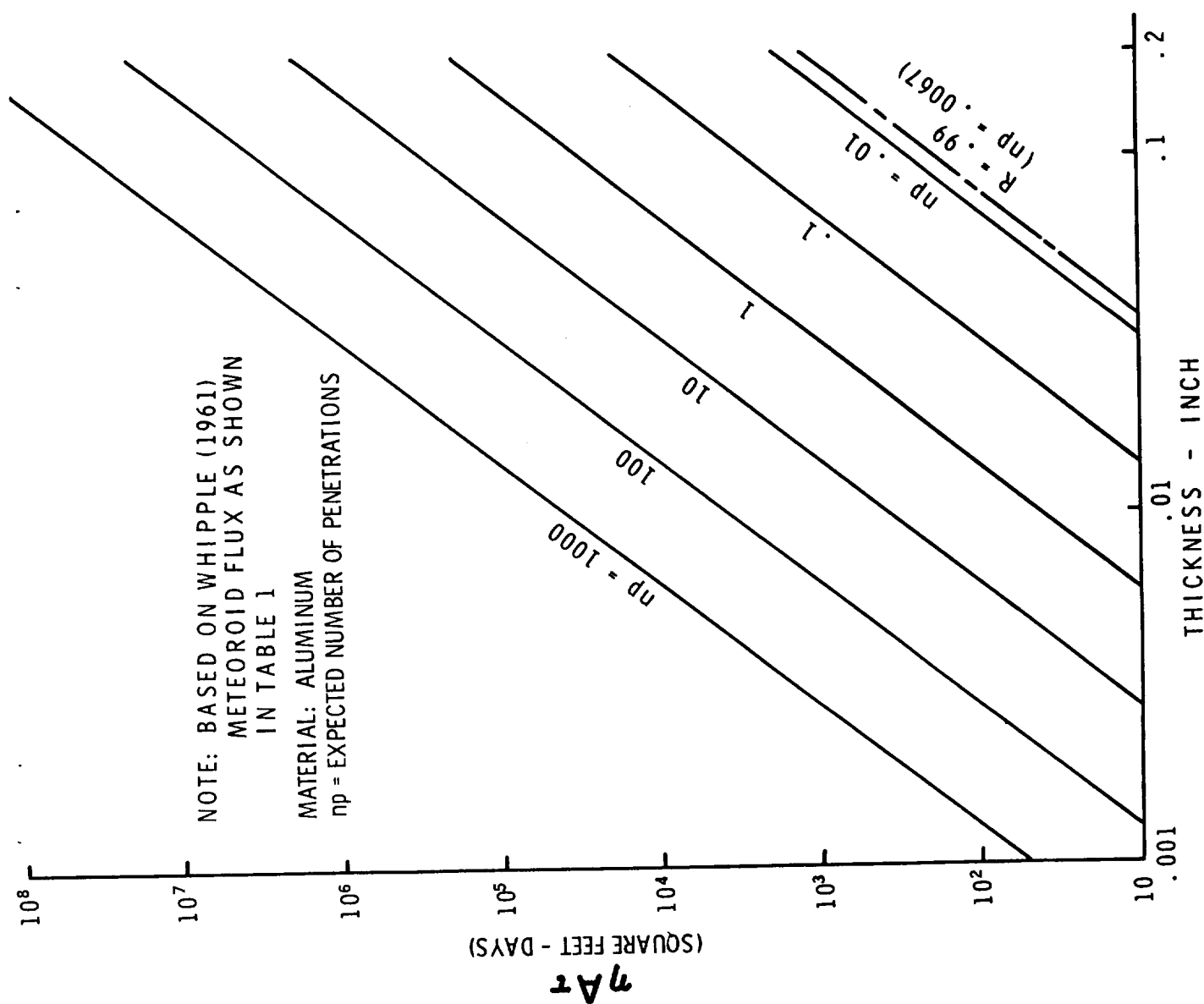Figure 8.   Histograms of expected number of penetrations

Figure 9. Thickness required for a given number of expected penetrations and exposure time.
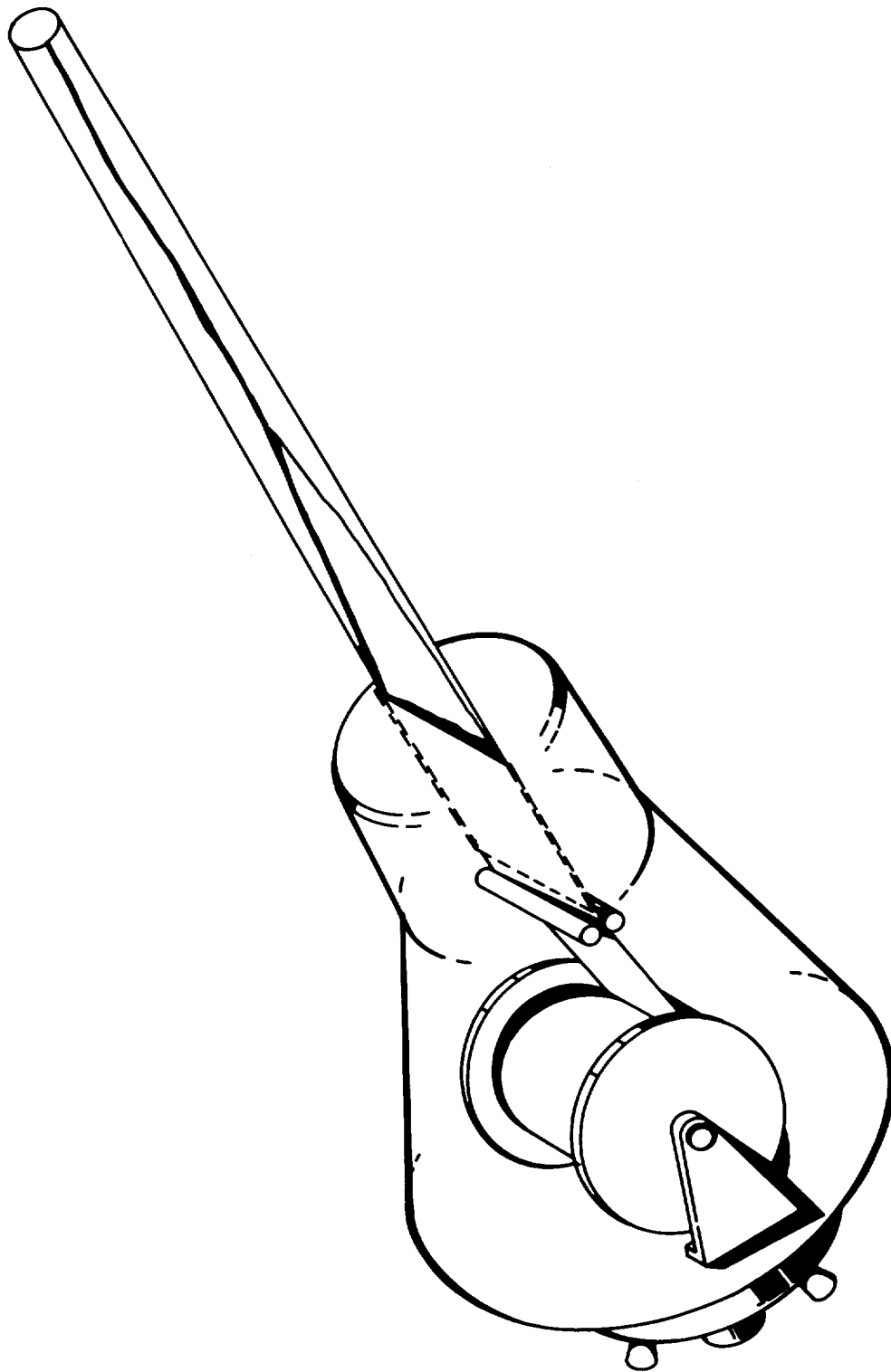
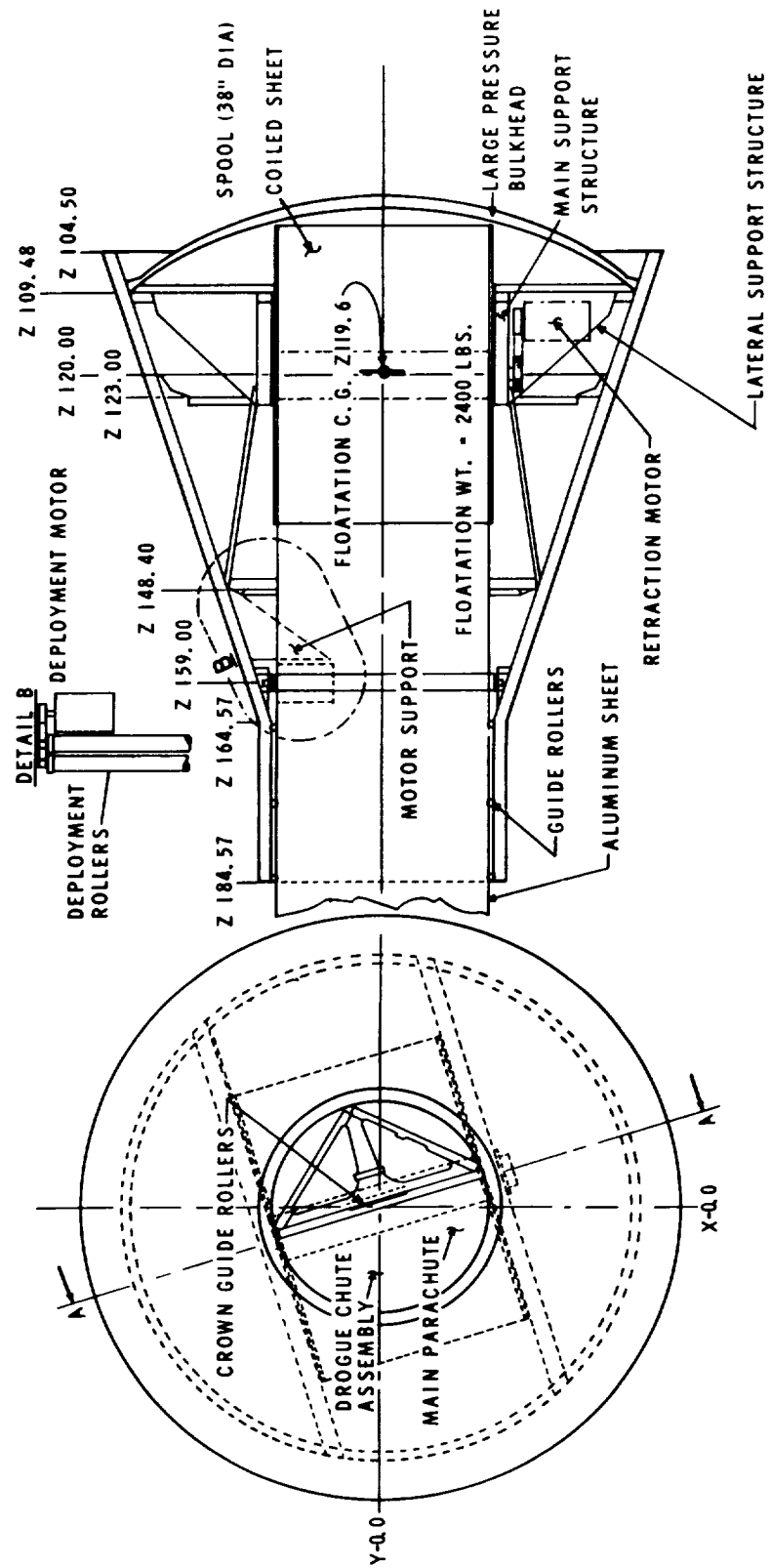Figure 10.   Artist's conception of sheet in extended position

Figure 11. Layout of coiled sheet within the spacecraft

(Sheet length = 1846 ft., t = .016", width = 26")

DESCRIPTION	WEIGHT	MOMENT ARM	MOMENT
STRUCTURE	817.06	123.58	100970.3
RECOVERY SYSTEM	25.91	156.6	4057.6
ATTITUDE CONTROLS	114.00	117.67	13414.0
RETRO SYSTEM	290.78	90.25	26243.0
LANDING SYSTEM	102.25	147.24	15055.3
TRACKING BEACON	19.11	123.91	2368.0
INSTRUMENTATION	28.04	123.56	3464.5
ELECTRICAL	106.00	113.93	12076.8
COMMUNICATIONS	13.76	116.28	1588.4
TEST SPECIMEN	1139.00	120.85	137645.0
ADAPTER	186.14	84.86	15796.4
LANDING BAG	141.45	102.39	14482.4
LAUNCH CONDITION	2983.3	116.37	347161.7
LESS ADAPTER	-186.14		-15796.4
ORBIT CONDITION	2797.16	118.46	331365.3
LESS JETTISONABLE ITEMS	-398.71		-44330.0
FLOTATION CONDITION	2398.45	119.68	287035.3

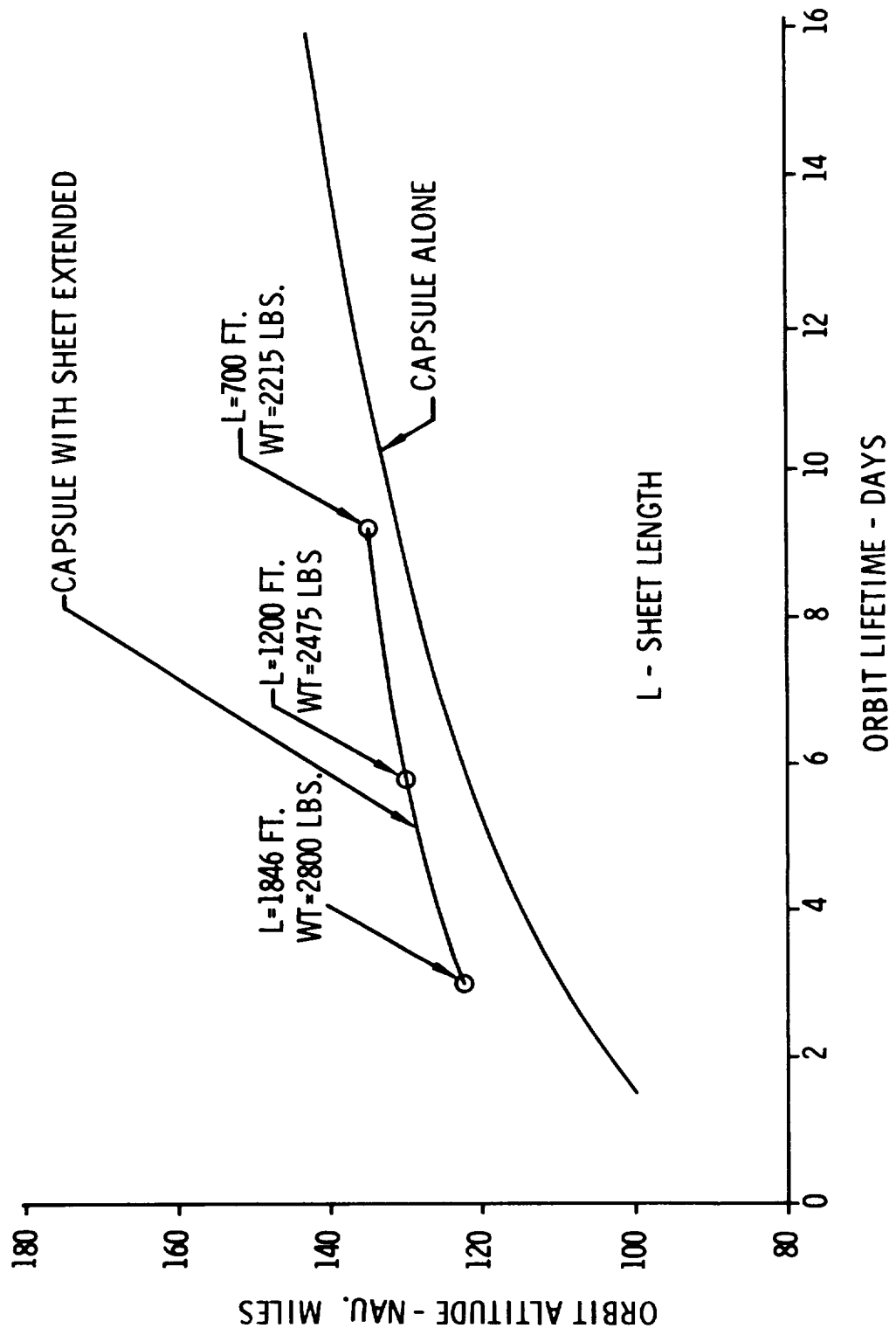Figure 12.   Summary weight and c. g. location

Figure 13. Lifetime in circular orbit
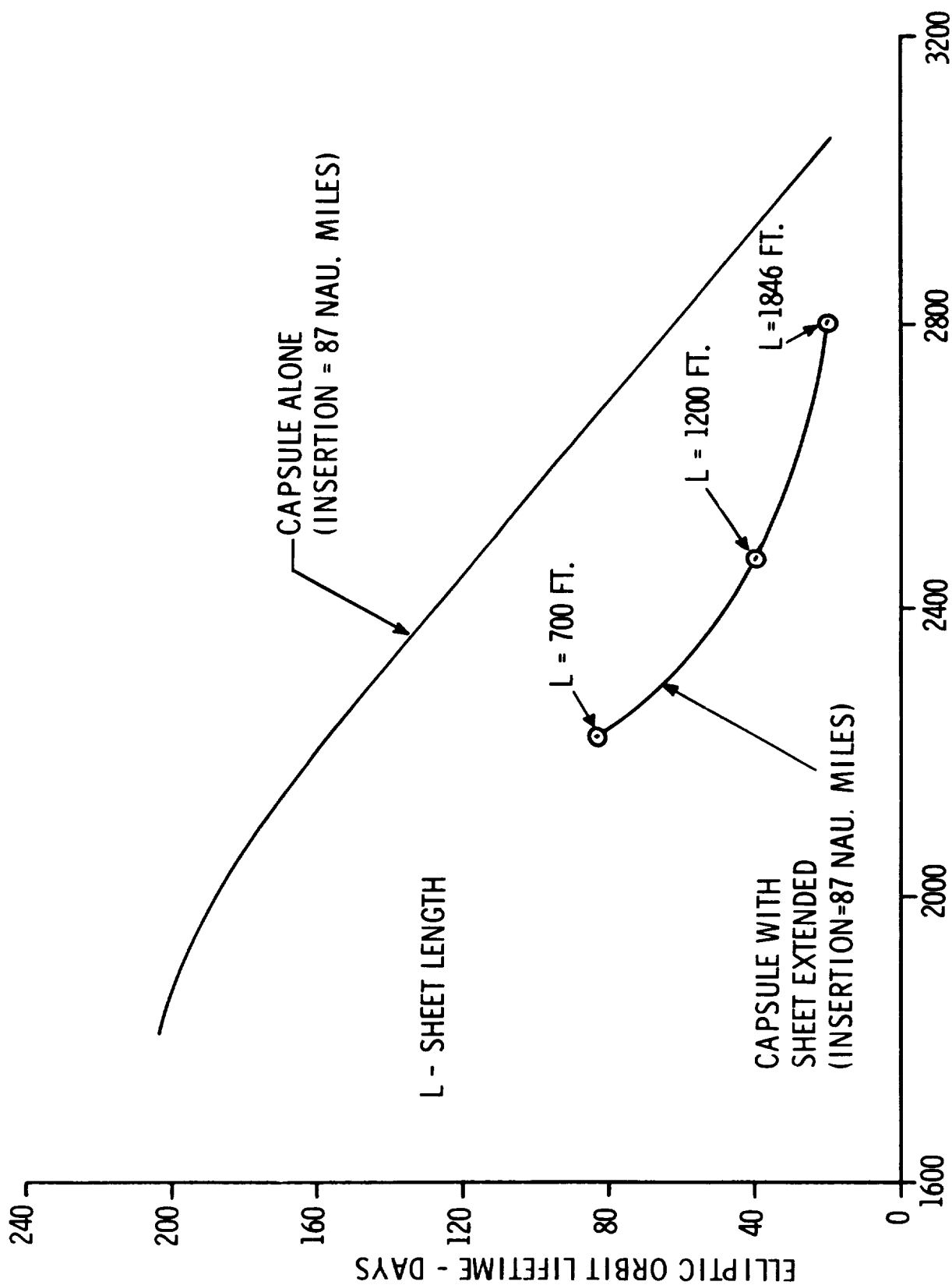
28

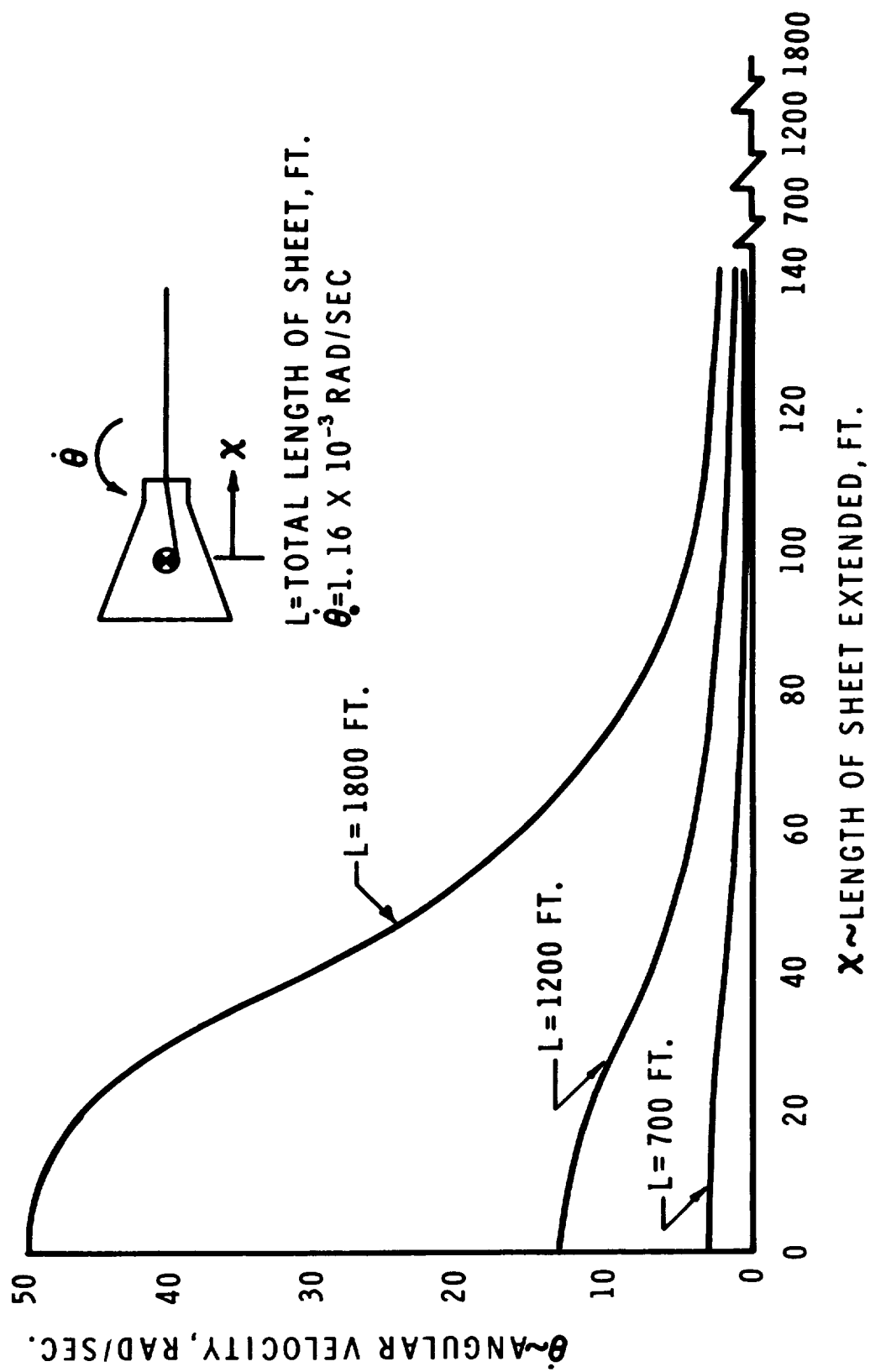Figure 14.   Lifetime for elliptic orbits

Figure 15.   Variation of angular velocity during retraction
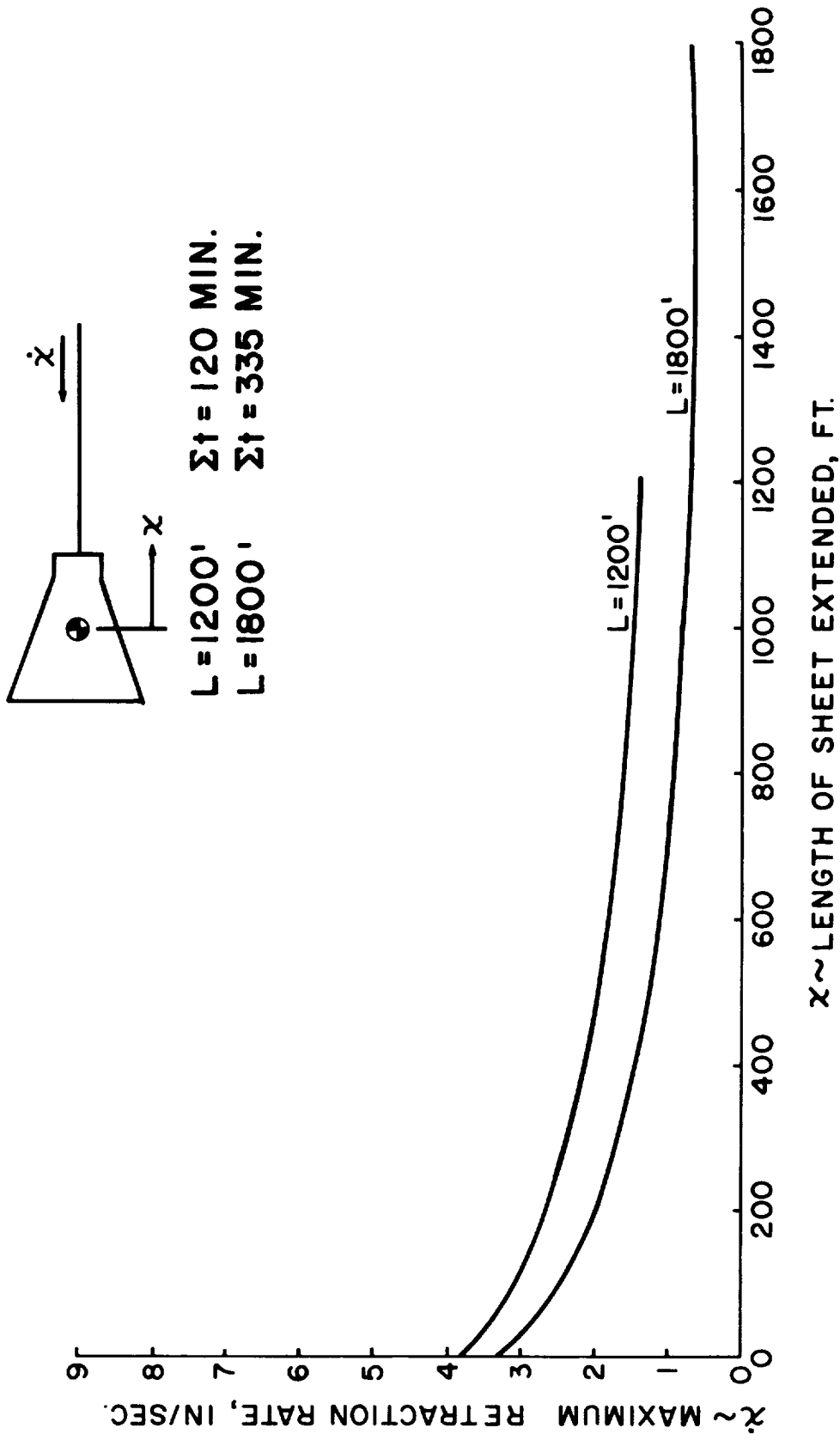
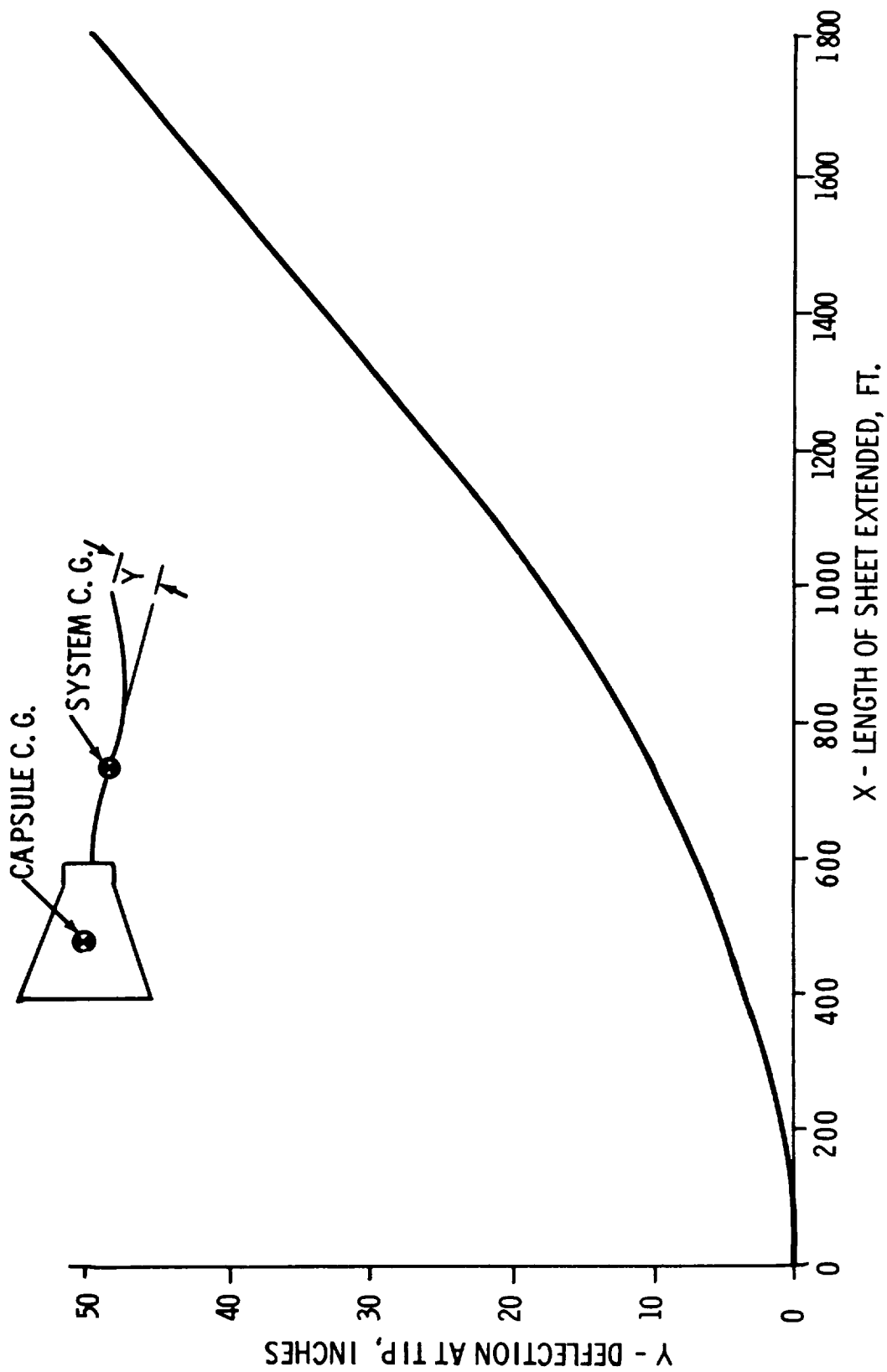Figure 16.   Limiting retraction rate to prevent buckling of sheet

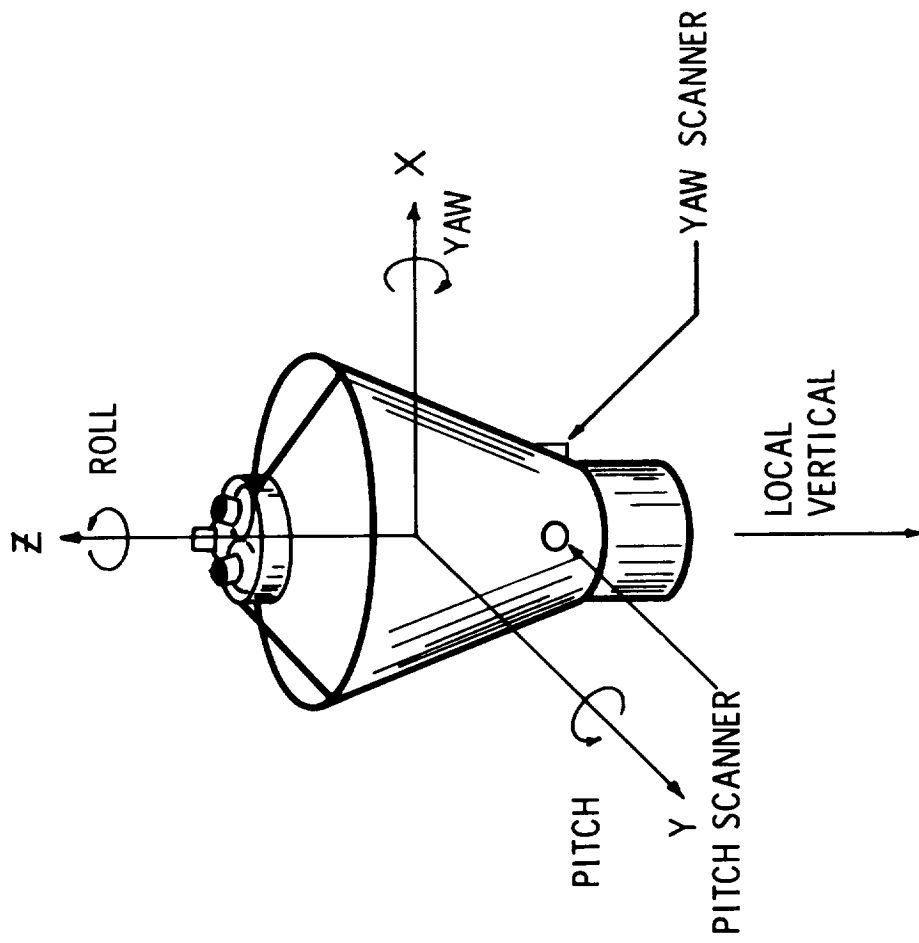Figure 17. Tip deflection at allowable retraction rate

Figure 18.   Retro-fire attitude – two-axis attitude control

VISUAL MAGNITUDE	MASS GRAMS	AVERAGE VELOCITY KM/SEC.	AVERAGE VELOCITY FT./SEC.
0	2.5	28	91,900
1	9.95×10^{-1}	28	91,900
2	3.96×10^{-1}	28	91,900
3	1.58×10^{-1}	28	91,900
4	6.28×10^{-2}	28	91,900
5	2.50×10^{-2}	28	91,900
6	9.95×10^{-3}	28	91,900
7	3.96×10^{-3}	28	91,900
8	1.58×10^{-3}	27	88,600
9	6.28×10^{-4}	26	85,300
10	2.50×10^{-4}	25	82,000
11	9.95×10^{-5}	24	78,700
12	3.96×10^{-5}	23	75,500
13	1.58×10^{-5}	22	72,200
14	6.28×10^{-6}	21	68,900
15	2.50×10^{-6}	20	65,600
16	9.95×10^{-7}	19	62,300
17	3.96×10^{-7}	18	59,100
18	1.58×10^{-7}	17	55,800
19	6.28×10^{-8}	16	52,500
20	2.50×10^{-8}	15	49,200

Table I. Relationship of meteroid velocity to visual magnitude

$\bar{t}_{al.}$ Ins.	N_P	m grams	np		
			$\eta A\tau = 30,000$	100,000	1,000,000
.010	2.4×10^{-2}	4.42×10^{-8}	720	2400	24,000
.016	5.7×10^{-3}	1.7×10^{-7}	171	570	5,700
.030	1.2×10^{-3}	1.0×10^{-6}	36	120	1,200
.060	1.6×10^{-4}	7×10^{-6}	6.4	16	160
.10	3.6×10^{-5}	2.95×10^{-5}	1.08	3.6	36
.17	8.0×10^{-6}	1.3×10^{-4}	.24	.8	8.0

Table II.   Effect of thickness on penetration data